Effect of Cross-Linking Agent on Curcumin Release from Chitosan-Based Macroparticles

Alessandro Pistone *, Annamaria de Gaetano, Elpida Piperopoulos, Chiara Abate

Posted Date: 18 July 2023

doi: 10.20944/preprints202307.1141.v1

Keywords: chitosan; curcumin; tripolyphophate; controlled-release drug system.

Article

Effect of Cross-Linking Agent on Curcumin Release from Chitosan-Based Macroparticles

Alessandro Pistone *, Annamaria de Gaetano, Elpida Piperopoulos and Chiara Abate

Department of Engineering, University of Messina, Contrada Di Dio, I-98166 Messina, Italy; annamaria.dg@hotmail.it (A.G.); elpida.piperopoulos@unime.it (E.P.); chiara.abate@unime.it (C.A.)

* Correspondence: alessandro.pistone@unime.it (A.P.); Tel.: +39-090-676-5506

Abstract: This work deals with the synthesis of bare and curcumin (CUR)-loaded chitosan (CS)-based macroparticles by ionic gelation using sodium hydroxide (NaOH) or sodium tripolyphosphate (TPP) as cross-linking agents. The resulting spherical-shaped macroparticles were studied using various characterization techniques, Scanning Electron Microscopy (SEM), Fourier Transformed Infrared Spectroscopy (FTIR), Thermogravimetric Analysis (TGA), and Differential Scanning Calorimetry (DSC). The release of CUR from the CS-based particles with respect to time was analyzed, and the encapsulation efficiency and degree of swelling were studied. All formulations showed excellent CUR trapping efficiency, exceeding 90%. In particular, the TPP-crosslinked macrobeads released 34 wt% of the charged CUR within minutes, while the remaining 66 wt% was released slowly due to the biodegradation of CS. The results indicate that the correct choice of gelling agent and its concentration leads to spherical particles capable of encapsulating CUR and releasing it in a wide range of kinetics depending on the specific application.

Keywords: chitosan; curcumin; tripolyphophate; controlled-release drug system

1. Introduction

Chitosan (CS), structurally composed of β-1,4-linked 2-amino-2-deoxy-β-D-glucose and N-acetyl-D-glucosamine units [1], is a natural derivative of chitin and the second most abundant polysaccharide after cellulose [2–4]. Among the various biopolymers, CS has attracted much attention for its remarkable biological and physical properties [4], and exhibits a wide variety of environmentally beneficial properties, such as abundant availability, biodegradability, non-toxicity, biocompatibility, recyclability, physiological inertness and cell adhesion, stability to air and moisture, and cost-effectiveness. It also possesses antitumor, mucoadhesive, immunostimulant, antifungal, antimicrobial, antibacterial, antioxidant, hemostatic, and wound healing properties [1–4], which make it an ideal candidate for pharmaceutical, and industrial applications [1,2,4–9]. In this context, CS can be employed as a recyclable green catalyst [5], in supercapacitors and biopolymer batteries, sensors, and water treatment [2,4]. It also finds wide use in cosmetics, food technology as food packaging, and in biomedical field, particularly in bioimaging, tissue engineering, wound dressing, and the textile industry, as well as in the design and development of drug delivery systems, implants, contact lenses and protein binding [1–4,10–12]. In particular, to design controlled release systems of CS-based drugs, the poor barrier and mechanical properties of CS can be modulated and improved by appropriately acting on the crosslinking process, and/or incorporating materials into CS films [3,6].

Once CS is solubilized in aqueous solutions under acid conditions, by protonation of its amine groups, it forms a gel in acetic acid, which can be precipitated in alkali to obtain spherical beads or physical hydrogels [6,8,13]. The use of some cross-linking reagents, such as sodium tripoliphosphate (TPP) is affordable because it involves an easy-to-prepare procedure and without toxic chemicals. In fact, TPP is a nontoxic multivalent anion forming crosslinks by ionic interaction between its negatively charged counter ion and the protonated amine groups of CS, improving the cross-linking

 doi:10.20944/preprints202307.1141.v1

density, particle size and zeta potential between CS and TPP, by adjusting their concentration, and the bioavailability, stability and controlled release of drugs; thus, showing promise as delivery systems for anticancer drugs, proteins, and nucleic acids [6,11,14,15].

The practical application of CS-based macro-, micro-, or nano-particles produced by ionic crosslinking is attracting attention both commercially and industrially [16] because of their intriguing properties for environmental applications, such as in catalytic processes [17,18], contaminant removal [13], probiotic encapsulation and release under acid conditions [19], and in biomedical field, where the design of CS-carriers is on the rise because CS behaves as an ideal pH-responsive and sensitive carrier for the delivery active ingredients due to the presence of positively charged pendant amino groups [10,16,20], and also it is able to encapsulate and release an active principle, such as curcumin.

Curcumin (CUR), an orange-yellow hydrophobic polyphenol derived from the rhizomes of the herb *Curcuma longa*, is another natural bioactive and therapeutic compound due to its anticarcinogenic, antibacterial, antimicrobial, antifungal, antiviral, antimalarial, antioxidant, antimutagenic, cicatrizing, anti-inflammatory, anti-coagulant, anti-fertility, antiprotozal, antifibrotic, antivenom, antiulcer, hypotensive, anticholesteremic properties, and free-radical effects [3,5,21–23]. Because of its flavoring properties, CUR is used as a food coloring, and as a traditional medicine in India and China for the treatment and prevention of several diseases, such as neurological, oncological, autoimmune, metabolic, cardiovascular, and diabetes, due to its extraordinary activities [3–5,22], which have attracted increasing interest from researchers to CUR [24]. However, the use of CUR in therapeutic applications has been limited due to its poor bioavailability and water-solubility [4,25,26]. In fact, CUR belongs to Class IV of Biopharmaceutics Classification System (BCS), whose solubility is about 7.8 $\mu g\ mL^{-1}$, and several preparative alternatives have been developed to improve its solubility, such as solid lipid nanoparticle, solid dispersion, colloidal drug delivery systems, microemulsion, and multicomponent crystal [23]. Encapsulation of CUR within materials, such as CS-based materials, is a strategic approach to improve its dispersibility in aqueous media, chemical stability, controlled release ability, bioactivity, and, thus, use in therapeutic treatment [4,25,27,28]. In addition, the combination of CUR with a biocompatible matrix, such as CS, enables the production of materials with unique and biologically interesting properties.

This work, aimed at developing pH-responsive CS-based beads via a simple, by-product-free dropping method, while also studying the effect of the crosslinking agent on CS-based particles, intends to at provide the proper insights for improving the bioavailability and controlled release of the active ingredient, CUR, in CS-based systems. This work also provides a promising avenue to construct highly biocompatible and biodegradable CS-based macrobeads for use in various practical applications.

2. Materials and Methods

2.1. Materials

Chitosan (CS, powder with molecular weight (MW): 200 $g\ mol^{-1}$ and deacetylated degree ≥ 90%) and sodium tripolyphosphate (TPP, MW: 367.86 $gmol^{-1}$, > 95%) were purchased by Glentham LIFE SCIENCES. Sodium hydroxide, pellets, reagent grade, Sharlau basic (MW: 40 $g\ mol^{-1}$, ≥ 97%) was also used.

Curcumin (CUR, powder with MW: 368.38 $g\ mol^{-1}$) was obtained from labfor. Ethanol (EtOH, MW: 46.07 $g\ mol^{-1}$, ≥ 97%) and Methanol (MW: 32.04 $g\ mol^{-1}$, ≥ 99.9%) were purchased from Honeywell Research Chemicals; acetic acid glacial (MW: 60.05 $g\ mol^{-1}$, ≥ 99.8%) and acetonitrile (MW: 41.053 $g\ mol^{-1}$, ≥ 99.9%) from Carlo Erba reagents. Hydrochloric acid (HCl, 37%) was also purchased from Sigma-Aldrich ACS reagent, and Phosphate Buffer (PBS, pH 7.2 at 25°C) from Sigma-Aldrich. Double deionized water (conductivity: < 0.1 $\mu S\ cm^{-1}$) was employed. All reagents were used without further purification.

Preprints (www.preprints.org) | NOT PEER-REVIEWED | Posted: 18 July 2023 doi:10.20944/preprints202307.1141.v1

2.2. Preparation of the CS- and CS- CUR- based macrobeads

Three different cross-linking media were used to gel the unloaded, CUR-loaded CS-based macroparticles: (a) 4 wt% NaOH in EtOH (26% v/v) solution (250 mL); (b) 2 wt% TPP and (c) 5 wt% TPP in aqueous solutions (250 mL).

In particular, 0.5 g of chitosan (CS) was gradually dissolved in 50 mL of an acetic acid solution (2%, v/v) under magnetic stirring for 3h at room temperature (rt). Then, the CS solution was dropped with a peristaltic pump (0.1 mL/min) into (a), (b), and (c) solutions under magnetic stirring (550 rpm). The obtained samples are denoted as CS-Na, CS-TPP2 and CS-TPP5, respectively, and shown in Table 1.

To prepare CS-based macroparticles with CUR, 0.5 g CS was dissolved in 50 mL of an acetic acid solution (2%, v/v) under magnetic stirring for 3h (rt). 0.1 g of CUR was completely dissolved in 25 mL of a mixture of acetonitrile:methanol (1:1 v/v), filtered and stored in the dark. Then, the CUR mixture was dropped into the CS solution and kept under magnetic stirring (550 rpm) for 30 minutes. The preparation procedure of the CUR-loaded CS-based macrospheres is similar to that of the unloaded samples described previously and shown in Figure 1. In more detail, the CS-based particles, loaded with CUR, prepared by precipitation in (a), (b), and (c) solutions, are CS-Na-CUR, CS-TPP2-CUR and CS-TPP5-CUR, respectively. All sample codes and their compositions are given in Table 1. After the cross-linking procedure, the macrobeads were sonicated for 1 h (rt), filtered and washed with double-distelled water to neutral pH. Finally, they stored at 4°C.

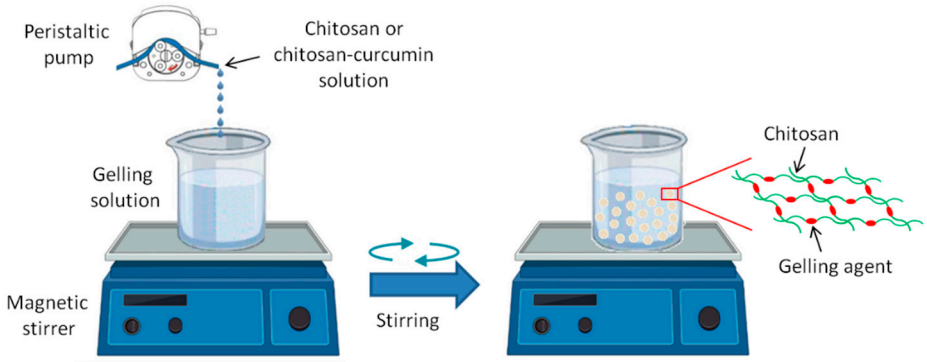

Figure 1. Scheme of chitosan (CS)-, and CS- curcumin (CUR)- macroparticles prepared by ionic gelation using NaOH or TPP as the gelling agent.

Table 1. Sample codes and composition of chitosan (CS)- based macroparticles.

Sample code	CS (g)	Cross-linking agent	CUR (g)
CS-Na	0.5	NaOH 4 wt%	-
CS-Na-CUR	0.5	NaOH 4 wt%	0.1
CS-TPP2	0.5	TPP 2 wt%	-
CS-TPP2-CUR	0.5	TPP 2 wt%	0.1
CS-TPP5	0.5	TPP 5 wt%	-
CS-TPP5-CUR	0.5	TPP 5 wt%	0.1

2.3. Characterization of the CS- and CS- CUR macrobeads

The prepared macroparticles were observed with an ECLIPSE *Si* Upright light Microscope (Nikon, type 104c), and analyzed by Scanning Electron Microscopy (SEM; FEI Quanta 450 equipment). The samples were completely dried (rt) and covered with a carbon coating to ensure good conductivity of the electron beam; then, photographs were taken with an accelerating voltage of 5 kV. The average diameter of the macroparticles was estimated by collecting more than 200 images in different areas of the samples.

 doi:10.20944/preprints202307.1141.v1

FTIR spectra were obtained with a Perkin Elmer spectrometer, Spectrum Two model. Spectra were previously collected by mixing a small amount of macroparticles with KBr and compressing them to form tablets. IR spectra were obtained in absorbance mode in the spectral region 4000-450 cm^{-1} with a resolution of 4 cm^{-1}.

Thermogravimetric studies were performed from 150 to 800 °C at 10 °C/min under argon on a TAQ500 instrument (TA Instruments, New Castle, DE, USA).

An SDT-Q 600 calorimeter (TA Instruments, New Castle, DE, USA) was used for DSC characterization. DSC curves were obtained using aluminum crucibles containing about 5 mg of samples under a nitrogen atmosphere (flow rate: 50 mL min^{-1}) from 50 to 400 °C at 10 °C/min. An empty aluminum crucible was used as a reference. The DSC cell was calibrated with indium (mp 156.6 °C; ΔH_{fusion} = 28.54 J g^{-1}) and zinc (mp 419.6 °C).

CUR encapsulation efficiency was measured by total dissolution of 50 g of macroparticles in 100 ml of HCl solution (0.1 mol L^{-1}). After filtration, the concentration of encapsulated CUR was determined on a Shimadzu UV-Vis spectrophotometer (model UV-2401 PC), set at 429 nm. A standard sample of CUR dissolved in a solution co of acetonitrile/methanol (1:1 v/v) was used to obtain the following calibration equation:

$$y = 4.8865x + 0.0273 \quad (1)$$

with R^2 = 0.9942, and where x is the CUR concentration (g L^{-1}) and y is the absorbance at 429 nm. Encapsulation efficiency was expressed as the percentage of encapsulated CUR relative to its total amount loaded into the CUR solution before the gelling step. Loading efficiency tests were assayed in triplicate for each sample.

CUR release kinetics were studied by suspending 50 g of macroparticles in 100 ml of PBS at pH 7.2 and 25 °C. At predetermined time intervals, 3 mL of sample was withdrawn to determine the quantity of dye released, and an equivalent amount of fresh dissolution medium was used to replace that removed. The samples were analyzed by UV-Vis spectrophotometry, as previously discussed. All experiments were performed in triplicate and the results were expressed as cumulative CUR release.

The swelling properties of the macroparticles were studied as gravimetrically measured water uptake by treating the macroparticles in doubly deionized water (pH 7) under gentle stirring for 120 min. The swollen samples were removed periodically (0, 5, 15, 30, 45, 60, 90 and 120 min), and their net weight was determined by weighing them, after previously removing the adsorbed water on the surface by blotting them with filter paper. Each swelling experiment was repeated twice, and the average value was taken as the swelling degree, calculated by the following formula:

$$\text{Swelling degree} = [(M_t - M_0)/M_t]\ 100 \quad (2)$$

where M_t is the weight of the swollen sample at time t, and M_0 is the initial weight of the sample before immersion in double-distilled water.

3. Results

3.1. Morphological Characterization of the macrobeads

The morphological properties of the CS- and CS- CUR- macroparticles were investigated. Figure 2 shows optical images and SEM micrographs of CS-based macroparticles crosslinked with NaOH, **(a)** CS-Na and CS-Na-CUR, as well as those with TPP **(b)** CS-TPP2 and CS-TPP2-CUR, compared with SEM micrographs of CS-TPP5 and CS-TPP5-CUR. All particles have a spherical shape and uniform size distribution. In particular, CS-Na and CS-TPP2 are white in color and have a better spherical distribution than the CUR-loaded macroparticles, which are yellow-brown. The optical images of CS-Na and CS-Na-CUR show a diameter of 2 mm, which decreases to 1 mm in those of CS-TPP2 and CS-TPP2-CUR. SEM analysis shows that all particles have a rough outer surface, and an increase in roughness was observed in CS-CUR particles, particularly CS-TPP-2. The macrobeads crosslinked with TPP also exhibit cavities with a very smooth inner surface.

Preprints (www.preprints.org) | NOT PEER-REVIEWED | Posted: 18 July 2023 doi:10.20944/preprints202307.1141.v1

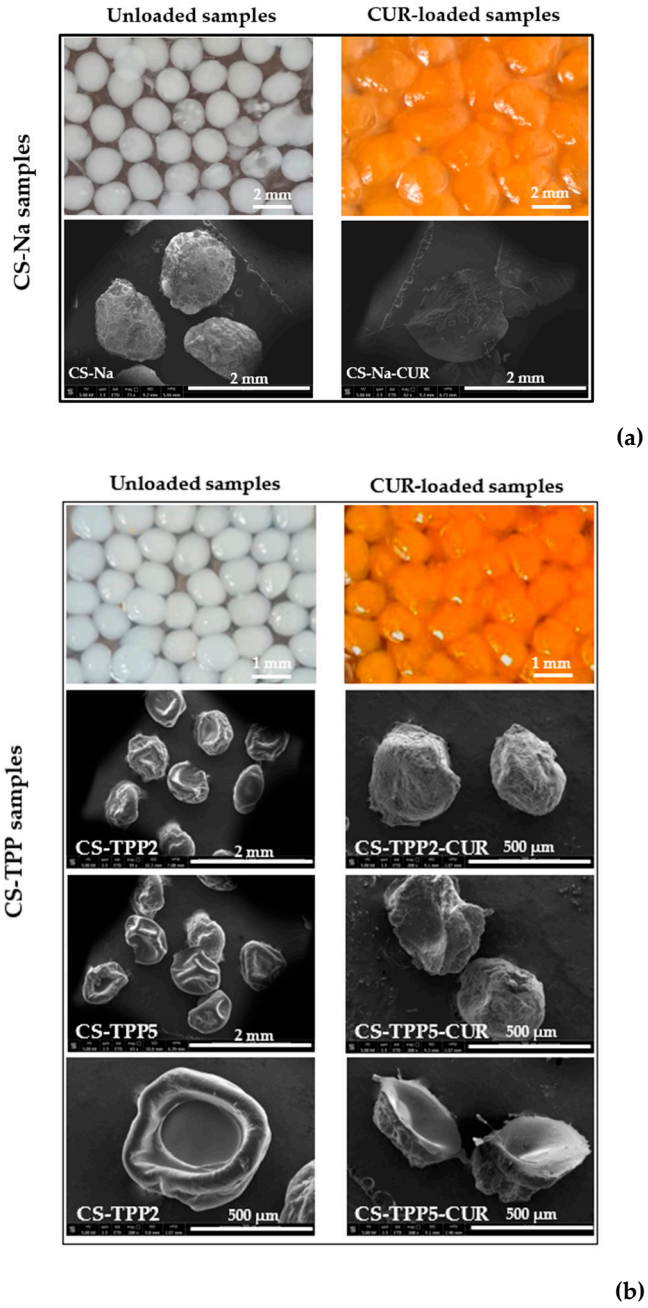

Figure 2. Optical images and SEM micrographs of CS-based macroparticles crosslinked with NaOH (**a**) CS-Na and CS-Na-CUR, and TPP (**b**) CS-TPP2, CS-TPP2-CUR, CS-TPP5 and CS-TPP5-CUR.

3.2. FTIR analyses

The structure of the CUR, CS and CS-CUR macroparticles, obtained in the different cross-linking media, was also confirmed by FTIR spectroscopy. Figure 3 shows the resulting FTIR spectra. The FTIR spectrum of CUR shows a characteristics broadband in the region between 3500-3200 cm^{-1}, due to the phenolic O-H stretching vibration, and the absorption band at 2900 cm^{-1}, referring to stretching vibration mode of C-H bond [29]. As previously reported in the literature [24,30], the peaks at 1630 cm^{-1} and 1600 cm^{-1} are assigned to the aromatic moiety C=C stretching, and the benzene ring stretching vibrations, respectively. At 1507 cm^{-1} the C=O and C=C vibrations occur, while the olefinic C-H bending vibrations are at 1429 cm^{-1}. The peaks at 1280 cm^{-1} and 1012 cm^{-1} are due to the asymmetrical stretching vibration of C–O-C and the symmetrical C–O–C stretching vibration of aryl alkyl ether, respectively [29,30]. The sharpest peaks located in the range of 700-900 cm^{-1} are attributable to the C-H deformation of alkene group [29].

Preprints (www.preprints.org) | NOT PEER-REVIEWED | Posted: 18 July 2023 doi:10.20944/preprints202307.1141.v1

The FTIR spectra for CS- macroparticles are different in the two cross-linking media investigated. In fact, the CS-Na spectrum shows characteristic absorption bands from 3000 to 3600 and at 2867 cm^{-1}, related to the presence of the OH and CH_3 groups, respectively. The peaks at 1659 cm^{-1} and 1569 cm^{-1} are attributable to the C=O stretching in the structure of N-acetylglucosamine and NH_2 stretching of glucosamine, respectively; the peak at 1420 cm^{-1} is due to the symmetrical carboxylate anion stretching [31]. The CS-TPP2 spectrum is very similar to that of the CS-TPP5 macroparticles, which is neglected in Figure 3 for simplicity. The FTIR spectrum of CS-TPP2 shows a stretching close to 1540 cm^{-1}, due to the interaction between phosphate groups and protonated CS [32,33], and additional stretching vibrations at 1218 and 1150 cm^{-1}, ascribable to the phosphate groups linked to the CSthrough intermolecular interactions [34,35].

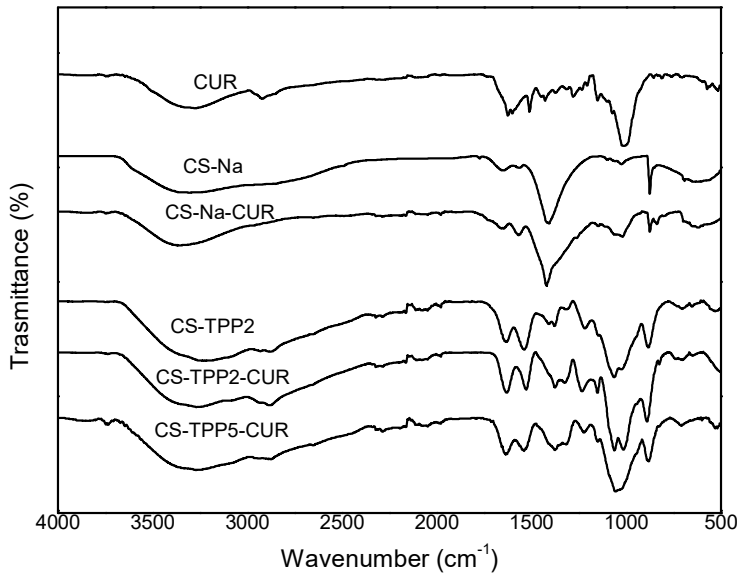

Figure 3. FTIR spectra of investigated samples.

3.3. TGA and DSC analyses

The thermal stability of CS-based macroparticles was studied by TGA analysis, under settings reported in Section 2.3. Figure 4 shows the profiles of CS-based macrobeads that, regardless of the type of gelling agent, have similar thermal degradation behavior. Two main steps of weight loss (%) were observed for all samples; the first, located at about 240 °C, is assigned to the dehydration of saccharide rings, and the second stage, at about 350 °C, is related to pyrolytic decomposition of the polymeric units with formation of the charcoal residues. Increasing the amount of TPP in the samples, a slight decrease in the thermal stability of the samples was observed. In fact, gelling with TPP led to a lowering of the thermal stability compared to the macrobeads obtaining with NaOH. Similar profiles have been reported by Laus et al. [33] and were attributed to a reduction in the crystallinity of the polymeric network formed by the cross-linked CSchains with bulky phosphate groups.

Preprints (www.preprints.org) | NOT PEER-REVIEWED | Posted: 18 July 2023 doi:10.20944/preprints202307.1141.v1

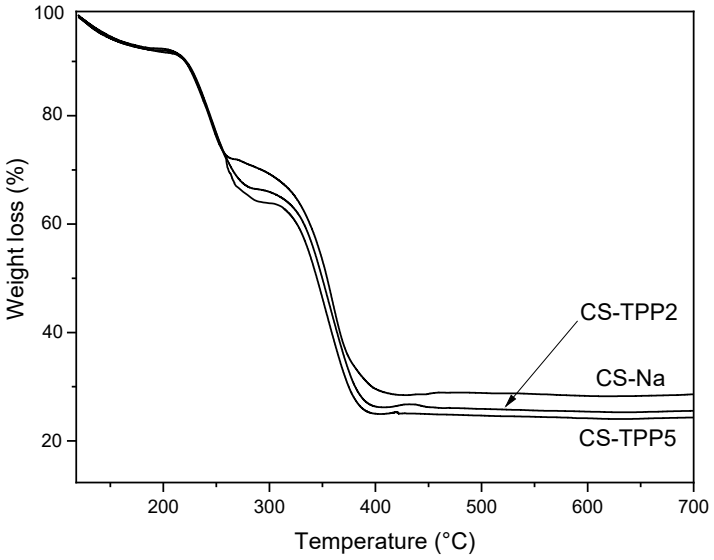

Figure 4. TGA analyses of the CS-based macrobeads.

DSC was employed to study the thermal effect of physical and chemical changes; Figure 5 reports the DSC curves of all the samples investigated. Pure CS shows heat absorption over a wide temperature range centered at 81.5 °C, due to the removal of physisorbed water. CS-based macrobeads crosslinked with NaOH or TPP exhibit an important endothermic signal at about 150 °C due to the glass transition temperature (T_g) of the CS-based biopolymer. In particular, the CS-based macrobeads crosslinked in TPP media display a slightly lower T_g than those cross-linked with NaOH, whose T_g value is 156.9 °C and drops to 146.7 °C in CS-TPP2 and 143.6 °C in CS-TPP5, respectively, indicating easier movement of the cross-linked CSchains. The addition of CUR leads to a further lowering of T_g, from 137.9 °C in CS-Na-CUR to 124.6 °C in CS-TPP2-CUR and 125.2 °C in CS-TPP5-CUR. This effect shows that CUR is trapped between the CS chains, thus acting as an additional spacer of the CS chains and facilitating their further mobility [36].

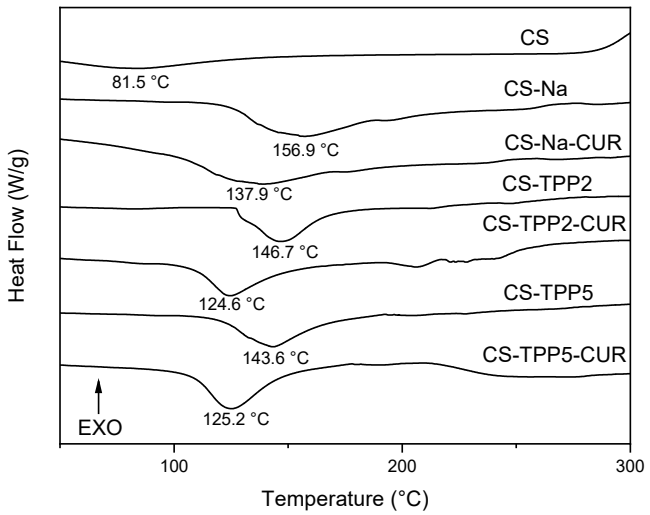

Figure 5. DSC curves of all investigated samples.

3.4. Evaluation of encapsulation and swelling degree of CUR

The encapsulation efficiency of CUR in the various CS-based macrobeads was measured as reported in Section 2.3, and the resulting data are listed in Table 2.

Preprints (www.preprints.org) | NOT PEER-REVIEWED | Posted: 18 July 2023 doi:10.20944/preprints202307.1141.v1

The results indicated that the loading efficiency was very high for all the samples, ranging from about 100 wt% using NaOH to 92-96 wt% with TPP as gelling agent. A slight decrease in encapsulation efficiency was observed with increasing TPP concentration in the gelling solution, from 95.9 wt% to 91.4 wt% for CS-TPP2-CUR and CS-TPP5-CUR, respectively. This decrease may be due to the amount of CUR trapped in the network of CSthat forms the particle walls rather than CUR remaining encapsulated in the inner cavity of the particles. An increase in the TPP concentration leads to a more cross-linked network within the particles walls, with more phosphate groups involved, which in turns hinders CUR encapsulation due to steric hindrances. This reduction in drug encapsulation efficiency in the CS/TPP system have already been observed [37–40].

Table 2. Encapsulation efficiency and swelling degree of CUR in the CS-based macroparticles.

Sample code	Encapsulation efficiency (wt%)	Swelling degree (wt%)
CS-Na-CUR	99.8	n.d.
CS-TPP2-CUR	95.9	120
CS-TPP5-CUR	91.4	90

n.d.: not detectable.

Figure 6 shows the effect of the different gelling agents on CUR release behavior. All samples analyzed showed a rapid release profile within minutes, but large differences were observed between particles obtained with NaOH or TPP as gelling agent. In particular, the CS-Na-CUR sample released 95 wt% of the loaded CUR within 5 minutes, reaching full release of the charged CUR at 120 minutes. The TPP-based samples showed a rapid release of about 27 wt% and 23 wt% of the loaded CUR within 5 minutes for CS-TPP2-CUR and CS-TPP5-CUR, respectively, followed by a slower release of no more than 34 wt% of loaded CURafter 2 days. Thus, the remaining amount of loaded CUR(66 wt%), which is strongly trapped within the CSchains or in the inner cavity of the particles, will be released with very slow kinetics at the same time as the biodegradation ofCS. Other authors have observed that increasing the concentration of the crosslinking agent leads to a decrease in the drug released due to the reduction of drug diffusion from the CS network [41].

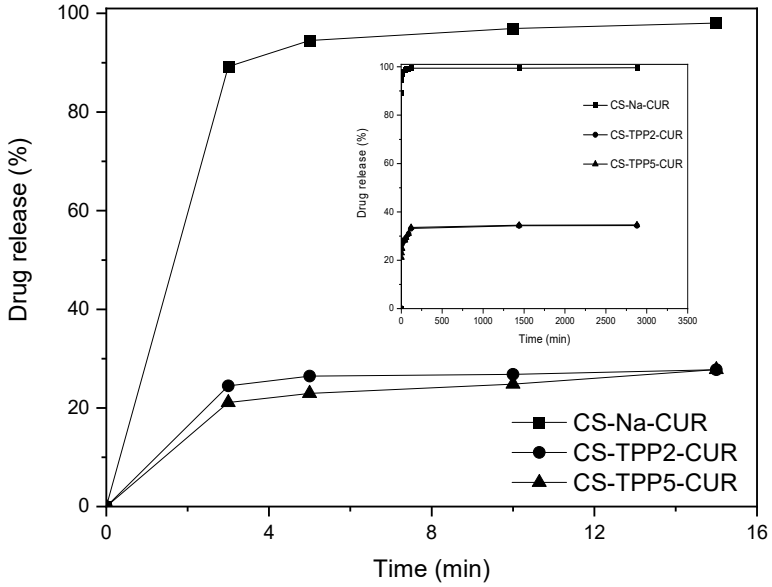

Figure 6. CUR release profiles of the macrobeads obtained with different gelling agents.

Table 2 also shows the swelling degree of the samples obtained with different crosslinking agents. In particular, the sample obtained with NaOH, as CS-Na-CUR, was unable to maintain its weight in water, showing a rapid degradation effect, and, therefore, it was difficult to fix a true degree

of swelling at equilibrium. For the samples obtained with TPP, the swelling ability decreased with increasing TPP concentration. These results suggest that a more tightly cross-linked CSmatrix does not swell as much as a poorly cross-linked CS matrix. The swelling behavior also reflects that of drug release; in fact, a higher swelling capacity means that water is better penetrated within the polymer matrix and, as a plasticizer, converts the glassy polymer to a more rubbery form and, consequently, leads to better drug release from the particle structure [42].

5. Conclusions

In the present work, spherical chitosan (CS)-based particles were synthesized by ionic gelation using due different cross-linking agents, NaOH and tripolyphosphate (TPP). The latter was employed at 2 wt% and 5 wt%, while NaOH 4 wt%. Under the same conditions, CS-based particles were loaded with curcumin (CUR). The obtaining macrobeads, namely CS-Na, CS-TPP2, CS-TPP5, CS-Na-CUR, CS-TPP2-CUR, and CS-TPP5-CUR, were characterized by SEM, FTIR, and TGA and DSC analyses. SEM confirmed the spherical morphology of the macroparticles, with a rough outer surface and a smooth inner cavity. The TGA and DSC analyses showed a slight decrease in the thermal stability of TPP-crosslinked samples compared with those cross-linked with NaOH. This effect is, influenced by the amount of TPP used. In particular, TGA analysis confirmed the encapsulation of CUR in the CS-based particles, showing a lowering of T_g, from 137.9 °C in CS-Na-CUR to 124.6 °C in CS-TPP2-CUR, and 125.2 °C in CS-TPP5-CUR. The DSC analysis further confirmed that CUR is trapped between the CS chains, acting as an additional spacer of the CS chains and facilitating their further mobility [36].

Ultimately, the encapsulation efficiency of CUR was more than 92 wt%. However, the NaOH cross-linked particles allow CUR to be released very quickly; while the TPP crosslinked samples released 34 wt% of the charged CUR within minutes, allowing the remaining 66 wt% to be released as a result of CS biodegradation.

Regarding the swelling behavior, CS-Na-CUR was unable to maintain its weight in water, showing rapid degradation, the samples obtained with TPP instead exhibited higher swelling ability, which decreased with increasing TPP concentration. These results suggest that a more tightly cross-linked CS matrix does not swell as much as a poorly cross-linked CS matrix, also reflecting drug release. In fact, higher swelling capacity means that water penetrates better within the polymer matrix and, as a plasticizer, converts the glassy polymer to a more rubbery form and, consequently, leads to better drug release from the particle structure [42].

The results indicate that the correct choice of gelling agent and its concentration leads to spherical particles capable of encapsulating CUR and releasing it in a wide spectrum of kinetics to be adopted according to specific applications.

Author Contributions: Conceptualization, A.P.; methodology, A.P. and A.G.; validation, A.P.; formal analysis, A.G. and E.P.; investigation, A.P. and A.G.; data curation, A.P. and C.A.; writing—original draft preparation, A.P. and A.G.; writing—review and editing, A.P. and C.A.; supervision, A.P.; project administration, NAVTEC (Consorzio di Ricerca per l'Innovazione tecnologica, Sicilia, Trasporti navali, commerciali e da diporto s.c.a.r.l); funding acquisition, A.P. All authors have read and agreed to the published version of the manuscript.

Funding: This research was funded by NAVTEC (Consorzio di Ricerca per l'Innovazione tecnologica, Sicilia, Trasporti navali, commerciali e da diporto s.c.a.r.l), name of project: SIMARE - Innovative Solutions for High Energy Saving Vessels; grant number 08ME7219090182 PO FESR 2014/2020 – Action 115"

Institutional Review Board Statement: Not applicable.

Informed Consent Statement: Not applicable.

Conflicts of Interest: The authors declare no conflict of interest.

References

1. Shariatinia, Z., Pharmaceutical applications of chitosan. *Advances in colloid and interface science* **2019,** 263, 131-194.
2. Dziedzic, I.; Kertmen, A., Methods of Chitosan Identification: History and Trends. *Letters in Applied NanoBioScience* **2023,** 12, (4), 94.
3. Madian, N. G.; El-Ashmanty, B. A.; Abdel-Rahim, H. K., Improvement of Chitosan Films Properties by Blending with Cellulose, Honey and Curcumin. *Polymers* **2023,** 15, (12), 2587.
4. Dhanavel, S.; Nivethaa, E. A. K.; Narayanan, V.; Stephen, A., In vitro cytotoxicity study of dual drug loaded chitosan/palladium nanocomposite towards HT-29 cancer cells. *Materials Science and Engineering: C* **2017,** 75, 1399-1410.
5. Lal, J.; Gupta, S. K.; Agarwal, D. D., Chitosan: An efficient biodegradable and recyclable green catalyst for one-pot synthesis of 3,4-dihydropyrimidinones of curcumin in aqueous media. *Catalysis Communications* **2012,** 27, 38-43.
6. Perez, J. J.; Francois, N. J.; Maroniche, G. A.; Borrajo, M. P.; Pereyra, M. A.; Creus, C. M., A novel, green, low-cost chitosan-starch hydrogel as potential delivery system for plant growth-promoting bacteria. *Carbohydrate Polymers* **2018,** 202, 409-417.
7. Dhanavel, S.; Praveena, P.; Narayanan, V.; Stephen, A., Chitosan/reduced graphene oxide/Pd nanocomposites for co-delivery of 5-fluorouracil and curcumin towards HT-29 colon cancer cells. *Polymer Bulletin* **2020,** 77, (11), 5681-5696.
8. Chen, X.; Wu, Y.-C.; Qian, L.-H.; Zhang, Y.-H.; Gong, P.-X.; Liu, W.; Li, H.-J., Fabrication of foxtail millet prolamin/caseinate/chitosan hydrochloride composite nanoparticles using antisolvent and pH-driven methods for curcumin delivery. *Food chemistry* **2023,** 404, 134604.
9. Chen, W.; Shen, X.; Hu, Y.; Xu, K.; Ran, Q.; Yu, Y.; Dai, L.; Yuan, Z.; Huang, L.; Shen, T.; Cai, K., Surface functionalization of titanium implants with chitosan-catechol conjugate for suppression of ROS-induced cells damage and improvement of osteogenesis. *Biomaterials* **2017,** 114, 82-96.
10. Yang, J.; Wang, Y.; Li, M.; Wu, H.; Zhen, T.; Xiong, L.; Sun, Q., pH-Sensitive Chitosan-Sodium Phytate Core-Shell Hollow Beads and Nanocapsules for the Encapsulation of Active Ingredients. *Journal of agricultural and food chemistry* **2019,** 67, (10), 2894-2905.
11. Soliman, G. M.; Zhang, Y. L.; Merle, G.; Cerruti, M.; Barralet, J., Hydrocaffeic acid-chitosan nanoparticles with enhanced stability, mucoadhesion and permeation properties. *European Journal of Pharmaceutics and Biopharmaceutics* **2014,** 88, (3), 1026-1037.
12. Wang, S.; Gao, Y.; Dong, L.; Chen, P.; Liu, W.; Yang, L., Cartilage-targeting and inflammatory-responsive nanocarriers for effective osteoarthritis treatment via reactive oxygen species scavenging and anti-angiogenesis. *Journal of Materials Science & Technology* **2023,** 143, 30-42.
13. Jagtap, S.; Thakre, D.; Wanjari, S.; Kamble, S.; Labhsetwar, N.; Rayalu, S., New modified chitosan-based adsorbent for defluoridation of water. *Journal of colloid and interface science* **2009,** 332, (2), 280-290.
14. Koukaras, E. N.; Papadimitriou, S. A.; Bikiaris, D. N.; Froudakis, G. E., Insight on the formation of chitosan nanoparticles through ionotropic gelation with tripolyphosphate. *Molecular pharmaceutics* **2012,** 9, (10), 2856-2862.
15. Gan, Q.; Wang, T.; Cochrane, C.; McCarron, P., Modulation of surface charge, particle size and morphological properties of chitosan-TPP nanoparticles intended for gene delivery. *Colloids and surfaces. B, Biointerfaces* **2005,** 44, (2-3), 65-73.
16. Tang, Y.; Wang, P.; Zeng, H.; Rui, Z., Construction of porous chitosan macrospheres via dual pore-forming strategy as host for alkaline protease immobilization with high activity and stability. *Carbohydrate Polymers* **2023,** 305, 120476.
17. Fajardo, H. V.; Martins, A. O.; de Almeida, R. M.; Noda, L. K.; Probst, L. F. D.; Carreño, N. L. V.; Valentini, A., Synthesis of mesoporous Al_2O_3 macrospheres using the biopolymer chitosan as a template: A novel active catalyst system for CO_2 reforming of methane. *Materials Letters* **2005,** 59, (29), 3963-3967.
18. Muresan, E. I.; Drobota, M.; Bargan, A.; Dumitriu, C. A. M., Hard porous chromium containing macrospheres as new catalysts for the esterification reaction of acetic acid with epichlorohydrin. *Central European Journal of Chemistry* **2014,** 12, (4), 528-536.
19. Luan, Q.; Zhang, H.; Wang, J.; Li, Y.; Gan, M.; Deng, Q.; Cai, L.; Tang, H.; Huang, F., Electrostatically reinforced and sealed nanocellulose-based macrosphere by alginate/chitosan multi-layer coatings for delivery of probiotics. *Food Hydrocolloids* **2023,** 142, 108804.

20. Liu, Y.; Cai, Z.; Ma, M.; Sheng, L.; Huang, X., Effect of eggshell membrane as porogen on the physicochemical structure and protease immobilization of chitosan-based macroparticles. *Carbohydrate Polymers* **2020,** 242, 116387.
21. Behbahani, E.; Ghaedi, M.; Abbaspour, M.; Rostamizadeh, K.; Dashtian, K., Curcumin loaded nanostructured lipid carriers: In vitro digestion and release studies. *Polyhedron* **2019,** 164, 113-122.
22. Mandal, D.; Sarkar, T.; Chakraborty, R., Critical Review on Nutritional, Bioactive, and Medicinal Potential of Spices and Herbs and Their Application in Food Fortification and Nanotechnology. *Applied biochemistry and biotechnology* **2023,** 195, (2), 1319-1513.
23. Fitriani, L.; Azizah, H.; Hasanah, U.; Zaini, E., ENHANCEMENT OF CURCUMIN SOLUBILITY AND DISSOLUTION BY ADSORPTION IN MESOPOROUS SBA-15. *International Journal of Applied Pharmaceutics* **2023,** 15, (1), 61-67.
24. Krishnan, V.; Venkatasubbu, G. D.; Kalaivani, T., Investigation of hemolysis and antibacterial analysis of curcumin-loaded mesoporous SiO_2 nanoparticles. *Applied Nanoscience* **2023,** 13, (1), 811-818.
25. Liang, F.; Wang, M.; Hu, Y.; Guo, Z.; Yang, W., Cetyltrimethylammonium bromide promoted dispersing and incorporation of curcumin into silica particles in alkaline ethanol/water mixture. *Colloids and Surfaces A: Physicochemical and Engineering Aspects* **2021,** 624, 126789.
26. Saputra, O. A.; Wibowo, F. R.; Lestari, W. W., High storage capacity of curcumin loaded onto hollow mesoporous silica nanoparticles prepared via improved hard-templating method optimized by Taguchi DoE. *Engineering Science and Technology, an International Journal* **2022,** 33, 101070.
27. Meng, W.; Sun, H.; Mu, T.; Garcia-Vaquero, M., Chitosan-based Pickering emulsion: A comprehensive review on their stabilizers, bioavailability, applications and regulations. *Carbohydrate Polymers* **2023,** 304, 120491.
28. El-Sherbiny, M.; Elekhtiar, R.; El-Hefnawy, M.; Mahrous, H.; Alhayyani, S.; Al-Goul, S.; Orif, M.; Tayel, A., Fabrication and assessment of potent anticancer nanoconjugates from chitosan nanoparticles, curcumin, and eugenol. *Frontiers in Bioengineering and Biotechnology* **2022,** 10, 1030936.
29. Ishak, N. A.; Hamidon, T. S.; Zi-Hui, T.; Hussin, M. H., Extracts of curcumin-incorporated hybrid sol–gel coatings for the corrosion mitigation of mild steel in 0.5 M HCl. *Journal of Coatings Technology and Research* **2020,** 17, (6), 1515-1535.
30. Yallapu, M. M.; Jaggi, M.; Chauhan, S. C., beta-Cyclodextrin-curcumin self-assembly enhances curcumin delivery in prostate cancer cells. *Colloids and surfaces. B, Biointerfaces* **2010,** 79, (1), 113-125.
31. Sharma, R. A.; Gescher, A. J.; Steward, W. P., Curcumin: the story so far. *European journal of cancer* **2005,** 41, (13), 1955-1968.
32. Xu, Y.; Du, Y., Effect of molecular structure of chitosan on protein delivery properties of chitosan nanoparticles. *International journal of pharmaceutics* **2003,** 250, (1), 215-226.
33. Laus, R.; Laranjeira, M. C. M.; Martins, A. O.; Fávere, V. T.; Pedrosa, R. C.; Benassi, J. C.; Geremias, R., MICROESFERAS DE QUITOSANA RETICULADAS COM TRIPOLIFOSFATO UTILIZADAS PARA REMOÇÃO DA ACIDEZ, FERRO(III) E MANGANÊS(II) DE ÁGUAS CONTAMINADAS PELA MINERAÇÃO DE CARVÃO. *Quimica Nova* **2006,** 29, (1), 34-39.
34. Lee, S.-T.; Mi, F.-L.; Shen, Y.-J.; Shyu, S.-S., Equilibrium and kinetic studies of copper(II) ion uptake by Chitosan-tripolyphosphate chelating resin. *Polymer* **2001,** 42, (5), 1879-1892.
35. Jain, A.; Jain, S. K., In vitro and cell uptake studies for targeting of ligand anchored nanoparticles for colon tumors. *European Journal of Pharmaceutical Sciences* **2008,** 35, (5), 404-416.
36. Parize, A.; Stulzer, H.; Laranjeira, M.; Brighente, I. I.; Souza, T., Evaluation of chitosan microparticles containing curcumin and crosslinked with sodium tripolyphosphate produced by spray drying. *Química Nova* **2012,** 35, (6), 1127-1132.
37. Desai, K. G.; Park, H., Preparation and characterization of drug-loaded chitosan-tripolyphosphate microspheres by spray drying. *Drug Development Research* **2005,** 64, (2), 114-128.
38. Desai, K. G.; Park, H. J., Encapsulation of vitamin C in tripolyphosphate cross-linked chitosan microspheres by spray drying. *Journal of microencapsulation* **2005,** 22, (2), 179-192.
39. Anal, A. K.; Stevens, W. F.; Remuñán-López, C., Ionotropic cross-linked chitosan microspheres for controlled release of ampicillin. *International journal of pharmaceutics* **2006,** 312, (1-2), 166-173.
40. Liu, C.; Desai, K. G.; Tang, X.; Chen, X., Drug Release Kinetics of Spray-Dried Chitosan Microspheres. *Drying Technology - DRY TECHNOL* **2006,** 24, (6), 769-776.

41. RemunanLopez, C.; Bodmeier, R., Mechanical, water uptake and permeability properties of crosslinked chitosan glutamate and alginate films. *Journal of Controlled Release* **1997,** 44, (2-3), 215-225.
42. Katas, H.; Hussain, Z.; Ling, T. C., Chitosan Nanoparticles as a Percutaneous Drug Delivery System for Hydrocortisone. *Journal of Nanomaterials* **2012,** 2012, 372725.